Hemisphere-specific optogenetic stimulation reveals left-right asymmetry of hippocampal plasticity

Michael M Kohl[1,2], Olivia A Shipton[1,2], Robert M Deacon[3], J Nicholas P Rawlins[3], Karl Deisseroth[4] & Ole Paulsen[1,2]

Postsynaptic spines at CA3-CA1 synapses differ in glutamate receptor composition according to the hemispheric origin of CA3 afferents. To study the functional consequences of this asymmetry, we used optogenetic tools to selectively stimulate axons of CA3 pyramidal cells originating in either left or right mouse hippocampus. We found that left CA3 input produced more long-term potentiation at CA1 synapses than right CA3 input as a result of differential expression of GluN2B subunit–containing NMDA receptors.

Hemispheric brain asymmetry has been the focus of numerous anatomical and psychological studies[1], and possible molecular correlates of such asymmetry have recently been identified in the mouse hippocampus[2–4]. It was found that postsynaptic spines of CA1 pyramidal cells targeted by projections from the right CA3 are larger and have higher GluA1, but lower GluN2B, expression than postsynaptic spines contacted by projections from the left CA3 (ref. 3). Given that changes in glutamate receptor distribution are thought to mediate long-term synaptic plasticity[5], we sought to investigate the effect of this hemispheric asymmetry on spike timing–dependent long-term potentiation (t-LTP)[6,7].

To selectively stimulate axons from either left or right CA3 pyramidal neurons, we made stereotactic injections of an adeno-associated virus containing a *loxP*-flanked inverted open reading frame (DIO) gene encoding a Channelrhodopsin2-eYFP (enhanced yellow fluorescent protein) fusion protein[8] (**Fig. 1a**) into either the left or right CA3 region in adult *Camk2a::cre* transgenic mice. This led to Cre-dependent, selective expression of Channelrhodopsin2-eYFP in cells positive for calcium/calmodulin-dependent kinase IIα (CamKIIα) (that is, excitatory cells) in the CA3 of one hippocampus and their ipsilateral and contralateral projections (Schaffer collateral and commissural fibers, respectively) (**Fig. 1b**,**c**). We prepared coronal slices of the hippocampal formation and obtained whole-cell recordings from CA1 pyramidal cells 14–28 d after injection (**Supplementary Methods**). Optical stimulation with 473-nm laser light in the stratum radiatum evoked reliable excitatory postsynaptic potentials (EPSPs) over the course of the experiment (EPSP slope remained stable for more than 50 min at 0.1-Hz stimulation, $n = 5$; **Supplementary Fig. 1**). These responses were comparable to EPSPs evoked by extracellular electrical stimulation, in that both were mediated by the generation of axonal action potentials

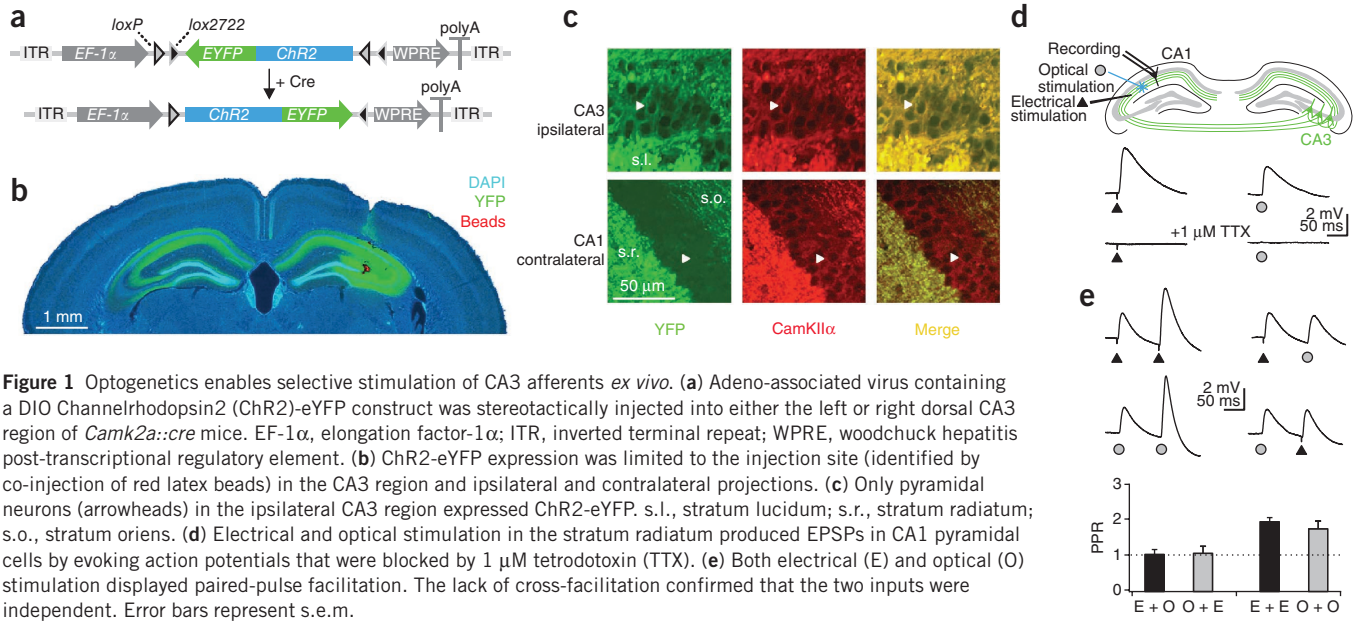

Figure 1 Optogenetics enables selective stimulation of CA3 afferents *ex vivo*. (**a**) Adeno-associated virus containing a DIO Channelrhodopsin2 (ChR2)-eYFP construct was stereotactically injected into either the left or right dorsal CA3 region of *Camk2a::cre* mice. EF-1α, elongation factor-1α; ITR, inverted terminal repeat; WPRE, woodchuck hepatitis post-transcriptional regulatory element. (**b**) ChR2-eYFP expression was limited to the injection site (identified by co-injection of red latex beads) in the CA3 region and ipsilateral and contralateral projections. (**c**) Only pyramidal neurons (arrowheads) in the ipsilateral CA3 region expressed ChR2-eYFP. s.l., stratum lucidum; s.r., stratum radiatum; s.o., stratum oriens. (**d**) Electrical and optical stimulation in the stratum radiatum produced EPSPs in CA1 pyramidal cells by evoking action potentials that were blocked by 1 μM tetrodotoxin (TTX). (**e**) Both electrical (E) and optical (O) stimulation displayed paired-pulse facilitation. The lack of cross-facilitation confirmed that the two inputs were independent. Error bars represent s.e.m.

[1]Department of Physiology, Development and Neuroscience, University of Cambridge, Cambridge, UK. [2]Department of Physiology, Anatomy and Genetics, University of Oxford, Oxford, UK. [3]Department of Experimental Psychology, University of Oxford, Oxford, UK. [4]Department of Bioengineering, Stanford University, Stanford, California, USA. Correspondence should be addressed to O.P. (op210@cam.ac.uk).

Received 8 April; accepted 21 July; published online 25 September 2011; corrected after print 13 October 2011; doi:10.1038/nn.2915

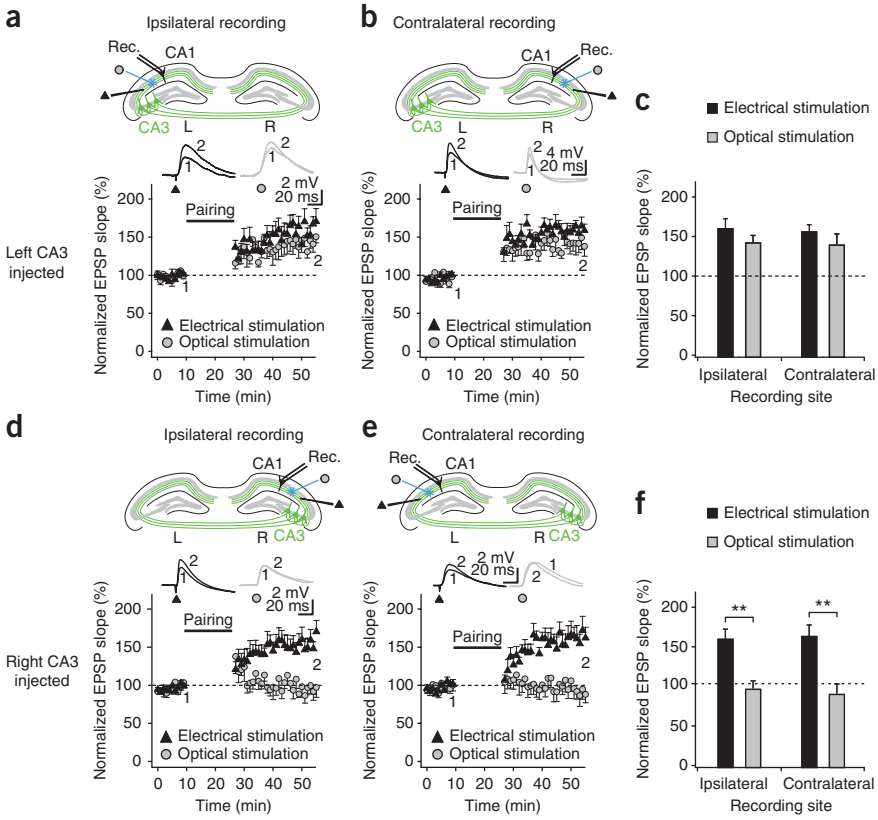

Figure 2 Hemispheric asymmetry of t-LTP at the CA3-CA1 pyramidal cell synapse. Indiscriminate electrical stimulation (triangles) in the stratum radiatum produced robust t-LTP in CA1 pyramidal neurons. (**a**–**c**) Selective optical stimulation (circles) of CA3 Schaffer collaterals (ipsilateral projections) and commissural fibers (contralateral projections) originating in the left hemisphere also both induced t-LTP. (**d**–**f**) In contrast, optical stimulation of CA3 projections originating in the right hemisphere led to significantly less t-LTP than electrical stimulation. Insets show representative EPSPs at the indicated time points (1, 2). Error bars represent s.e.m. $^{**}P < 0.01$, Student's *t* test.

(>99% EPSP block by 1 μM tetrodotoxin, n = 4; **Fig. 1d**) and showed similar paired-pulse ratios ($PPR_{electrical}$, 2.0 ± 0.1, n = 18; $PPR_{optical}$, 1.8 ± 0.2, n = 17; **Fig. 1e**). Optical and electrical stimulation consistently recruited independent inputs, as no cross-facilitation was observed ($PPR_{electrical\text{-}optical}$, 1.1 ± 0.1, n = 6; $PPR_{optical\text{-}electrical}$, 1.1 ± 0.2, n = 6; **Fig. 1e**).

We next investigated t-LTP at the CA3-CA1 synapse, monitoring EPSPs evoked by alternating optical and electrical stimulation in the stratum radiatum. Although electrical stimulation activates fibers irrespective of their hemispheric origin, optical stimulation specifically recruits fibers from the injected CA3. To guard against the possible effects of different expression patterns or levels following left and right injection, we induced t-LTP under equivalent conditions by adjusting light intensity and electrical current to produce similar sized EPSPs (2–4 mV), and using a burst pairing protocol[7] with simultaneous activation of electrical and optical input. Pairing consisted of presynaptic stimulation followed 5–10 ms later by a postsynaptic burst of action potentials and was repeated 100 times (**Supplementary Methods**). There was a significant difference in the magnitude of t-LTP induced depending on the hemispheric origin of afferent fibers. In slices prepared from left-injected animals, pairing elicited robust t-LTP in the optically evoked input (144 ± 8%, n = 14; $P < 0.01$, Student's *t* test), whereas slices from right-injected animals showed no t-LTP in the optical pathway (93 ± 8%, n = 14, P = 0.37, Student's *t* test). Consistent with earlier reports[9,10], this was not caused by possible differences between ipsilateral and contralateral pathways, as we found t-LTP of equivalent magnitude in the ipsilateral and contralateral optical pathway in slices from left-injected mice (ipsilateral, 145 ± 9%, n = 7; contralateral, 142 ± 13%, n = 7; **Fig. 2a**–**c**). In contrast, we found no t-LTP in either optical pathway in right-injected mice (ipsilateral, 96 ± 10%, n = 7; contralateral, 90 ± 12%, n = 7; **Fig. 2d**–**f**). There were no significant differences between the electrical pathways (left-injected: ipsilateral, 164 ± 12%, n = 7; contralateral, 160 ± 8%, n = 7; right-injected: ipsilateral, 159 ± 12%, n = 7; contralateral, 163 ± 14%, n = 7; $F_{3,24}$ = 0.04, P = 0.99, ANOVA).

To exclude the possibility that this left-right difference was a result of an induction threshold effect, we repeated the experiments with a stronger pairing protocol in the hippocampus contralateral to the

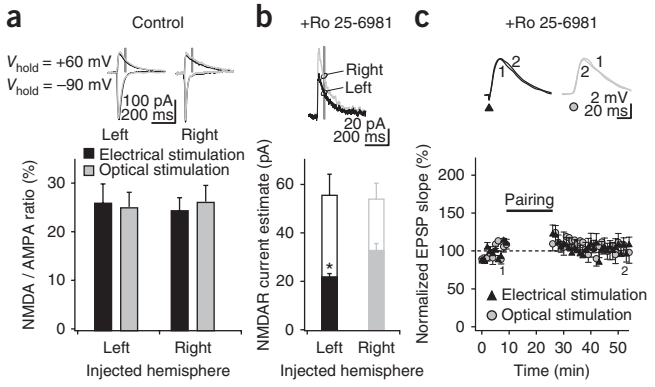

Figure 3 Asymmetric expression of GluN2B-containing NMDARs underlies hemispheric differences in t-LTP. (**a**) Hemisphere-selective optical stimulation (gray traces, gray bars) and hemisphere-indiscriminate electrical stimulation (black traces, black bars) of afferents from CA3 were used to evoke postsynaptic currents in CA1 pyramidal cells contralateral to the injection side. There was no difference in the overall NMDA/AMPA ratios between left and right for either electrical or optical stimulation (dark gray box indicates the time window for estimation of the NMDAR current). (**b**) Selective block of GluN2B subunit–containing NMDARs with 0.5 μM Ro 25-6981 affected the NMDAR current evoked by left CA3 input more than that evoked by right CA3 input. Open bars indicate NMDAR current estimate in control, filled bars indicate remaining NMDAR current in the presence of 0.5 μM Ro 25-6981. Traces show representative optically evoked postsynaptic currents at +60 mV in the presence of 0.5 μM Ro 25-6981 for left- and right-injected animals. (**c**) 0.5 μM Ro 25-6981 completely blocked t-LTP in CA1 cells receiving left CA3 (optical stimulation, circles) or mixed CA3 inputs (electrical stimulation, triangles). Insets show representative EPSPs at the indicated time points (1, 2). Error bars represent s.e.m. $^{*}P < 0.05$, Student's *t* test.

injection side and the experimenter blind to injection side, producing equivalent results (optical pathway: left-injected, 142 ± 20%, $n = 6$; right-injected, 111 ± 12%, $n = 6$; electrical pathway: left-injected, 150 ± 15%, $n = 6$; right-injected, 169 ± 19%, $n = 6$; **Supplementary Fig. 2**).

Subsequently, we wanted to examine a possible mechanism underlying this asymmetry in t-LTP. NMDA receptor (NMDAR) activation is known to be required for induction of LTP[6]; we therefore first tested whether CA1 cells showed a difference in NMDAR/AMPA receptor (AMPAR)-mediated current ratio (NMDA/AMPA ratio) depending on the hemispheric origin of their presynaptic input from CA3. However, they did not: the overall NMDA/AMPA ratio was not different with respect to input (left-injected: optical stimulation, 23 ± 3%; electrical stimulation, 26 ± 4%; right-injected: optical, 27 ± 3%, electrical, 25 ± 2%; $n = 6$; **Fig. 3a**). Nevertheless, there was an NMDAR subunit–dependent difference between the two sides: the selective GluN2B subunit antagonist Ro 25-6981 (0.5 µM) blocked 60% of the total NMDAR current from left CA3 inputs compared with 38% of the total NMDAR current from right CA3 inputs (left-injected: Ro 25-6981, 22 ± 1 pA; control, 55 ± 9 pA, $n = 6$; right-injected: Ro 25-6981, 33 ± 3 pA; control, 53 ± 7 pA; $n = 7$; **Fig. 3b**). To test whether this difference could explain why left CA3 input displays more t-LTP, we repeated pairing experiments in the presence of 0.5 µM Ro 25-6981. t-LTP in left-injected animals was completely blocked under these conditions (**Fig. 3c**), suggesting that the difference in GluN2B subunit expression is sufficient to explain the hemispheric asymmetry in t-LTP. Similar to electrical pairing–induced t-LTP, optically evoked t-LTP is most likely expressed postsynaptically, as we observed no change in PPRs following t-LTP induction (**Supplementary Table 1**).

In summary, using optogenetic tools for cell type– and hemisphere-specific recruitment of CA3 axons, we found that inputs from the left CA3 onto CA1 pyramidal cells are more able to produce t-LTP than inputs from the right CA3. This hemispheric asymmetry in plasticity could be explained by differential GluN2B expression at synapses targeted by the left and right CA3 (ref. 3), consistent with recent evidence suggesting that GluN2B subunit–containing NMDARs favor LTP induction[11,12]. Given that cortical NMDAR subunit expression appears to be regulated by activity-dependent mechanisms[12–14], this result raises the possibility that the left and right CA3 might be differentially active and hence produce input-specific differences in postsynaptic spines, consistent with recent morphological observations that spines receiving input from right CA3 are more mature than those receiving left CA3 input[3]. The behavioral consequences of the hemisphere-specific asymmetry in synaptic plasticity that we found remain to be investigated, but such experiments are now possible using optogenetic control of neuronal activity *in vivo*[15].

Note: Supplementary information is available on the Nature Neuroscience website.

ACKNOWLEDGMENTS

The authors would like to thank D. Paterson for providing surgery facilities, and D. Kätzel and L. Upton for help with immunohistochemistry. This research was supported by the Biotechnology and Biological Sciences Research Council and the Wellcome Trust (OXION Initiative). An equipment grant from the EPA Cephalosporin Fund is gratefully acknowledged.

AUTHOR CONTRIBUTIONS

M.M.K. conducted the experiments and analyzed the data. O.A.S. contributed recordings. M.M.K. and R.M.D. injected the animals. J.N.P.R. provided advice on the project. K.D. designed and cloned the AAV DIO ChR2-YFP vector. M.M.K. and O.P. designed the experiments. M.M.K., O.A.S. and O.P. wrote the manuscript.

COMPETING FINANCIAL INTERESTS

The authors declare no competing financial interests.

Published online at http://www.nature.com/natureneuroscience/.
Reprints and permissions information is available online at http://www.nature.com/reprints/index.html.

1. Toga, A.W. & Thompson, P.M. *Nat. Rev. Neurosci.* **4**, 37–48 (2003).
2. Wu, Y. *et al. J. Neurosci.* **25**, 9213–9226 (2005).
3. Shinohara, Y. *et al. Proc. Natl. Acad. Sci. USA* **105**, 19498–19503 (2008).
4. Kawakami, R. *et al. Science* **300**, 990–994 (2003).
5. Malinow, R. & Malenka, R.C. *Annu. Rev. Neurosci.* **25**, 103–126 (2002).
6. Bliss, T.V. & Collingridge, G.L. *Nature* **361**, 31–39 (1993).
7. Pike, F.G., Meredith, R.M., Olding, A.W. & Paulsen, O. *J. Physiol. (Lond.)* **518**, 571–576 (1999).
8. Sohal, V.S., Zhang, F., Yizhar, O. & Deisseroth, K. *Nature* **459**, 698–702 (2009).
9. Bliss, T.V.P., Lancaster, B. & Wheal, H.V. *J. Physiol. (Lond.)* **341**, 617–626 (1983).
10. Wheal, H.V., Lancaster, B. & Bliss, T.V.P. *Brain Res.* **272**, 247–253 (1983).
11. Barria, A. & Malinow, R. *Neuron* **48**, 289–301 (2005).
12. Yashiro, K. & Philpot, B.D. *Neuropharmacology* **55**, 1081–1094 (2008).
13. Hoffmann, H., Gremme, T., Hatt, H. & Gottman, K. *J. Neurochem.* **75**, 1590–1599 (2000).
14. Mierau, S.B., Meredith, R.M., Upton, A.L. & Paulsen, O. *Proc. Natl. Acad. Sci. USA* **101**, 15518–15523 (2004).
15. Aravanis, A.M. *et al. J. Neural Eng.* **4**, S143–S156 (2007).

Corrigendum: Hemisphere-specific optogenetic stimulation reveals left-right asymmetry of hippocampal plasticity

Michael M Kohl, Olivia A Shipton, Robert M Deacon, J Nicholas P Rawlins, Karl Deisseroth & Ole Paulsen
***Nat. Neurosci.* 14, 1413–1415 (2011); published online 25 September 2011; corrected after print 13 October 2011**

In the version of this article initially published, the schematics, traces and graphs in Figures 2d and 2e were interchanged. The error has been corrected in the HTML and PDF versions of this article.

Supplementary Information

Hemisphere-specific optogenetic stimulation reveals left-right asymmetry of hippocampal plasticity

Michael M. Kohl, Olivia A. Shipton, Robert M. Deacon, J. Nicholas P. Rawlins, Karl Deisseroth, Ole Paulsen

Contents:

Nature Neuroscience: doi:10.1038/nn.2915

Supplementary Figures

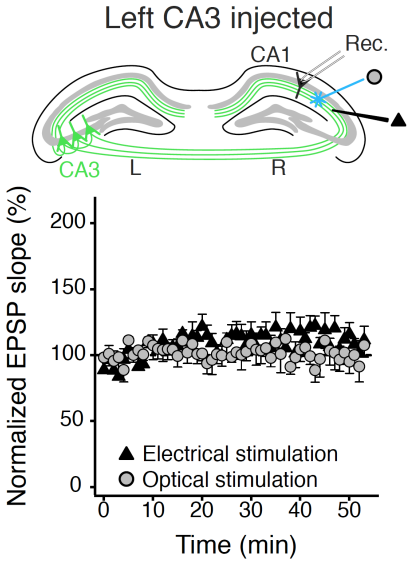

Supplementary Figure 1 Stability of electrically and optically-evoked synaptic responses. Current-clamp recordings from CA1 pyramidal cells on the contralateral side of left-injected mice. Electrical stimulation (triangles) and optical stimulation (circles) were delivered in the stratum radiatum (n = 5). EPSPs stabilized 18–20 minutes after establishment of whole-cell configuration and remained stable for more than 50 minutes recording time. Error bars are s.e.m.

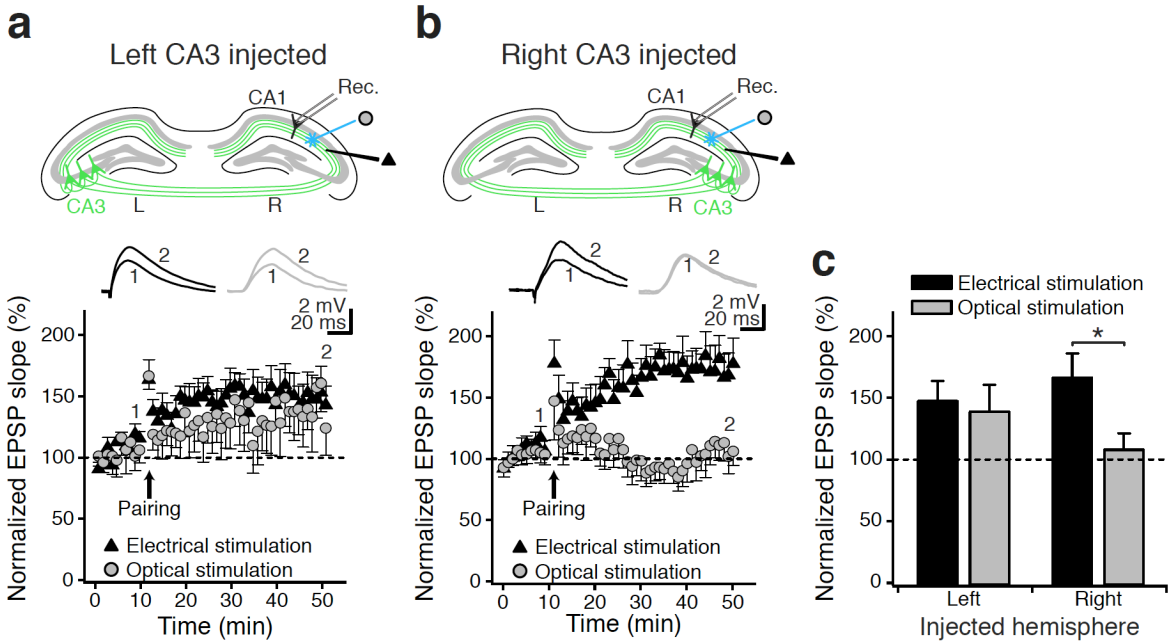

Supplementary Figure 2 Asymmetric induction of t-LTP at the CA3–CA1 pyramidal cell synapse with a strong pairing protocol. (**a, b**) With the experimenter blind to injection side, a stronger pairing paradigm consisting of 4 x 10 burst pairings at 5 Hz produced robust t-LTP in CA1 pyramidal neurons for electrical stimulation (triangles) in the stratum radiatum regardless of injection side. In contrast, hemisphere-selective optical stimulation of commissural fibers (circles) yielded robust t-LTP for left- but not right-injected mice. (**c**) Summary of results. Error bars are s.e.m. * $P < 0.05$, Student's *t*-test.

Nature Neuroscience: doi:10.1038/nn.2915

Supplementary Table 1 Paired-pulse ratios before and after t-LTP pairing protocol.

	Left				**Right**			
	Ipsi		**Contra**		**Ipsi**		**Contra**	
	Electric	*Light*	*Electric*	*Light*	*Electric*	*Light*	*Electric*	*Light*
n	6	6	5	5	6	5	5	5
Pre-pairing	1.9 ± 0.1	1.6 ±0.3	2.0 ± 0.5	1.6 ± 0.4	1.9 ± 0.2	1.7 ± 0.2	2.0 ± 0.1	1.9 ± 0.6
Post-pairing	2.0 ± 0.1	1.7 ± 0.1	1.8 ± 0.4	1.4 ± 0.4	1.9 ± 0.2	1.6 ± 0.3	1.9 ± 0.2	1.7 ± 0.3
% change	3.5 ± 6.8	16.6 ± 13.7	–6.6 ± 6.9	–15.7 ± 11.8	6.8 ± 9.6	–5.9 ± 7.9	–5.2 ± 4.0	7.2 ± 19.2

Supplementary Materials & Methods

Animals and AAV vectors

All procedures were carried out in accordance with British Home Office regulations. *CamKIIα::cre* mice[16] were obtained from Jackson Laboratories. ChR2 was fused to the fluorescent protein eYFP and cloned in the antisense direction into pAAV-MCS (Stratagene) to create AAV DIO ChR2-eYFP (for a vector outline and sequence see http://www.optogenetics.org). ChR2-eYFP was flanked by a pair of canonical loxP sites and a pair of mutated lox2272 sites, which are inverted by Cre to enable transcription from the EF-1α promotor. A woodchuck hepatitis B virus post-transcriptional element was placed in the sense direction 5' of the poly(A). Adeno-associated viral particles of serotype 2 were produced by the Vector Core Facility at The University of North Carolina at Chapel Hill.

Virus injections

CamKIIα-cre mice (5–10 weeks old) were anesthetized with 2–4% isoflurane at 0.6–1.4 min^{-1}. A small craniotomy was made 1.5 mm anterior and 2.2 mm lateral (either left or right) from interaural zero. Through a small durotomy, 0.1 µl fluorescent bead suspension (Molecular Probes) and 0.4 µl virus suspension (AAV DIO ChR2-eYFP, 4 x 10^{12} viral molecules ml^{-1}) were delivered at a rate of 0.1 µl min^{-1} 2.25 mm below the skull surface through a 33-gauge needle using a Hamilton Microliter syringe. Following a 5 minute wait after bolus injection, the needle was retracted by 0.2 mm and after another 5 minutes slowly retracted fully. The scalp incision was sutured, and post-injection analgesics and anti-inflammatory drugs (5 mg kg^{-1} meloxicam) were administered intraperitoneally to aid recovery.

Immunohistochemistry

Mice were anesthetized by intraperitoneal injection of 100 µl ketamine (100 mg ml^{-1}; Fort Dodge) and 50 µl medetomidin (1 mg ml^{-1}; Pfizer) and then transcardially perfused with phosphate-buffered saline (PBS, pH 7.4) containing 4% (wv^{-1}) paraformaldehyde (PFA) and 0.2% (wv^{-1}) picric acid. Brains were post-fixed for 24 hours at 4 °C in perfusion solution and subsequently infiltrated with 30% (wv^{-1}) sucrose in PBS for at least 24 hours. Coronal sections of 60 µm thickness were cut using a Leica SM 2000R sliding microtome. Sections were rinsed three times in Tris-buffered saline (TBS, Sigma), three times in TBS containing 3% (wv^{-1}) Triton X-100 (TBS-T), and once for 1 hour in TBS-T containing 20% (vv^{-1}) horse serum (Vector Labs) and then incubated for 48 hours at 4 °C in TBS-T containing 1% horse serum and anti-GFP (rabbit, 1:500, Sigma) and anti-Cre recombinase (mouse, 1:500,

Nature Neuroscience: doi:10.1038/nn.2915

Millipore) antibodies, as well as 0.0001% DAPI (Sigma). The sections were rinsed four times in TBS and stained in TBS-T containing 1% horse serum and Alexa488- and Alexa546-labeled secondary antibodies (Invitrogen). After four rinses in TBS, slices were mounted in VectaShield (Vector Labs) and imaged on a Leica TCS SP2 confocal microscope.

Slice preparation and electrophysiology

Fourteen–28 days post-injection, mice were decapitated under deep isoflurane anesthesia and coronal slices of the hippocampal formation (350 μm) were prepared under low-light conditions. Slices were maintained submerged in oxygenated (95% O_2, 5% CO_2) artificial cerebrospinal fluid (aCSF) containing (in mM): 126 NaCl, 3 KCl, 1.25 NaH_2PO_4, 2 $MgSO_4$, 2 $CaCl_2$, 26 $NaHCO_3$, and 10 glucose, pH 7.2-7.4. After recovering at room temperature (22-27 °C) for at least one hour, slices were transferred to the recording chamber and superfused with aCSF, bubbled with 95% O_2, 5% CO_2, at 1–2 ml min^{-1}. Cells with a pyramidal-shaped soma in the stratum pyramidale of CA1 were selected for recording using infrared, differential interference contrast optics[17].

Whole-cell patch-clamp recordings were performed with glass pipettes (3–5 MΩ for voltage-clamp, 5–7 MΩ for current-clamp), pulled from standard borosilicate glass. In voltage-clamp experiments the pipette solution contained (in mM): CsCl 140; EGTA 0.2; HEPES 10.0; ATP-Mg 2.0; GTP-NaCl 0.3; QX-314 5.0, adjusted to pH 7.2; osmolarity 280–290 mosmol l^{-1}). Voltage-clamp experiments were performed in the presence of gabazine (3 μM) with afferents from CA3 cut, and recordings were started after allowing at least 10 minutes for the intracellular solution to diffuse following breakthrough. Stimulation strength was adjusted to yield 150–200 pA EPSC peak amplitude at –90 mV.

In current-clamp experiments the pipette solution contained (in mM): 110 potassium-gluconate, 40 HEPES, 2 ATP-Mg, 0.3 GTP, 4 NaCl (pH 7.2–7.3; osmolarity 270–290 mosmol l^{-1}). In current-clamp recordings all cells were tested for regular spiking responses to positive current injection. Excitatory postsynaptic potentials (EPSPs) were evoked in the stratum radiatum at 0.1 or 0.2 Hz, alternating between an extracellular stainless steel electrode (20–60 μs, 150–350 μA) and a blue laser spot (473 nm, 5 ms, 1–5 mW at objective entry using a single mode fiber for laser-microscope coupling; UGA-40, Rapp OptoElectronic). Responses typically stabilized within 18–20 minutes, and then both electrical and optical pathway reliably produced stable EPSPs of equal magnitude over more than 35 minutes (**Supplementary Fig. 1**). To avoid intracellular wash-out we used only a 10 minute baseline after breakthrough and before pairing, and rejected recordings where the average EPSP slope for early (t = 0 to 3 min) and late (t = 7 to 10 min) baseline changed by > 10%. Two pairing protocols were used. One protocol consisted of simultaneous electrical and optical stimulation followed 5–10 ms later by a postsynaptic burst of action potentials and was repeated 100 times at baseline frequency. The other consisted of pairing simultaneous electrical and optical stimulation followed 5–10 ms later by a postsynaptic burst of action potentials 10 times at 5 Hz and repeating this train four times at 10 s intervals[8]. Data were low-pass filtered at 2 kHz and acquired at 5 kHz with a Molecular Devices Axon Multiclamp 700B amplifier (current clamp in bridge-mode). The signal was recorded on a PC using the Axon pClamp 9 acquisition software. Cells were rejected if series resistance changed by more than 20% during the course of the experiment. Data for t-LTP induced by the theta burst induction protocol (**Supplementary Fig. 2**) and all voltage-clamp experiments were collected and analyzed blind to injection side.

Nature Neuroscience: doi:10.1038/nn.2915

Data analysis

All analysis was performed using custom-made procedures in Igor Pro (Wavemetrics, OR, USA). Plasticity was assessed from the slope of the EPSP, measured on the rising phase of the monosynaptic EPSP as a linear fit between time points corresponding to 20% and 80% of the peak amplitude during baseline conditions. For statistical comparisons, the mean EPSP slope was averaged over the three minutes immediately before pairing and 27–30 minutes after pairing. Paired-pulse ratios were obtained from 6 consecutive recordings just before pairing and 30 minutes after pairing. The NMDA/AMPA receptor-mediated current ratio (NMDA/AMPA ratio) was calculated as described previously[14]. In brief, the AMPA receptor-mediated peak current was measured at a holding potential of –90 mV. The NMDA receptor-mediated current was estimated as the average current amplitude at a holding potential of +60 mV between 50 ms and 60 ms after the peak AMPA current. The NMDA/AMPA ratio was calculated by dividing the NMDA current estimate by the peak AMPA current at –90 mV. The liquid-junction potential was not compensated for. Representative traces are averages of 10 (voltage-clamp) or 5 (current-clamp) consecutive recordings. Statistical comparisons were made using one- and two-sample Student's *t*-test as appropriate. P-values less than 0.05 were considered significant. Data are presented as mean ± s.e.m.

Supplementary References

16. Hinds, H.L., Goussakov, I., Nakazawa, K., Tonegawa, S. & Bolshakov, V.Y. *Proc Natl Acad Sci USA* **100**, 4275-4280 (2003).

17. Stuart, G.J., Dodt, H.U. & Sakmann, B. *Pflugers Arch* **423**, 511-518 (1993).

Nature Neuroscience: doi:10.1038/nn.2915